

Electron transport in shock ignition targets

A.R. Bell^{1,2}

¹ Clarendon Laboratory, University of Oxford, Parks Road, Oxford OX1 3PU, UK

² STFC Central Laser Facility, Rutherford Appleton Laboratory, Oxfordshire, OX11 0QX, UK

Shock ignition [1, 2] is one of the most promising routes to commercially viable inertial fusion energy (IFE). In common with fast ignition and its variants, the two processes of (i) fuel compression and (ii) heating to ignition temperature are separated. Compression is achieved on a low adiabat with minimum energy input. Once compressed, a strong shock is launched into the target by a high power laser. The shock converges on the centre of the target, heating the target, and initiating ignition. Betti et al [1] investigate target designs which require a compression laser pulse energy of about 250kJ delivered in about 5 nsec and an ignition laser pulse of about 100kJ delivered in 100-300psec. The total laser energy requirement is significantly less than that of conventional IFE in which heating results from compression at high velocity. The ignition laser intensity reaches $\sim 6 \times 10^{15} \text{ Wcm}^{-2}$. At this high intensity, some energy is delivered to high energy electrons, but this is beneficial since even 100keV electrons contribute positively to shock formation at high density in the compressed target. Fast electron preheat is less of a concern since the target is already compressed. The large laser energy delivered in a short pulse also produces high temperatures over short distances, and the target does not have time to relax to quasi-steady ablation. Strong temperature gradients and large heat flows occur. During the shock ignition pulse, the Spitzer thermal conductivity may be invalid, and a non-local transport treatment may be necessary.

We show here that laser interaction with dense targets during shock ignition can be separated into two regimes. In the ablative regime, corresponding to conditions found in conventional directly driven IFE, the interaction relaxes to a quasi-steady balance between electron thermal conduction carrying energy to high density and hydrodynamic energy flux (ablative enthalpy flow) which carries energy away from high density. In contrast, at high laser intensity, the energy flux into the target is too great to be balanced by hydrodynamic flow. In this regime, the structure is that of a supersonic heat front with very little hydrodynamic response. In a calculation assuming that the Spitzer conductivity is acceptably valid, we show that conditions during shock ignition straddle the boundary between these two regimes.

When reduced to its bare essentials, the laser-plasma interaction can be represented by 1D perfect gas fluid equations for mass, momentum and energy with additional energy fluxes

carried by the laser and by Spitzer conduction (I and $Q = -\kappa_s \nabla T$ respectively).

$$\begin{aligned}\frac{\partial \rho}{\partial t} &= -\frac{\partial(\rho u)}{\partial x} \\ \frac{\partial(\rho u)}{\partial t} &= -\frac{\partial(\rho u^2)}{\partial x} - \frac{\partial P}{\partial x} \\ \frac{\partial}{\partial t} \left(\frac{3}{2}P + \frac{1}{2}\rho u^2 \right) &= -\frac{\partial}{\partial x} \left(\frac{5}{2}Pu + \frac{1}{2}\rho u^3 - \kappa_s \frac{\partial T}{\partial x} + I \right)\end{aligned}$$

These equations have a self-similar solution with a form which depends on the dependence of the conductivity on fluid variables. The Spitzer conductivity is determined by the mean free path λ of electrons as can be shown by writing the Spitzer heat flow as

$$Q = q \frac{\lambda}{L_T} n_e k_B T \left(\frac{k_B T}{m_e} \right)^{1/2}$$

where L_T is the temperature scalelength $L_T = T/|\nabla T|$, $Q_f = n_e k_B T (k_B T/m_e)^{1/2}$ is the free-streaming heat flow, and q is a numerical factor of order unity. For Coulomb collisions, $\lambda \propto T^2$, and this results in a self-similar solution which depends on a scaled distance $s = x/t^{4/3}$. ρ , u , P , Q & I can then be written as functions of s times a power of the ratio of time t to some characteristic time t_0 :

$$\begin{aligned}\rho &= \rho(s) \quad ; \quad u = \mu(s) \left(\frac{t}{t_0} \right)^{1/3} \quad ; \quad P = \rho(s) \phi(s) \left(\frac{t}{t_0} \right)^{2/3} \\ Q &= - \left(\frac{\kappa_0}{t_0^{4/3}} \right) \phi^{5/2} \frac{\partial \phi}{\partial s} \left(\frac{t}{t_0} \right) \quad ; \quad I = \varepsilon(s) \left(\frac{t}{t_0} \right)\end{aligned}$$

where κ_0 is a constant determining the magnitude of the Spitzer heat flow. ε is the self-similar laser energy flux. For laser energy absorption at a particular position s_{abs} , with a delta function energy input to the plasma where the density is $\rho(s_{abs})$, ε is a constant for $s < s_{abs}$, and $\varepsilon = 0$ for $s > s_{abs}$. The self-similar hydro equations in the overdense plasma ($I = 0$) are then:

$$\begin{aligned}\frac{\partial}{\partial s} (\rho \mu) &= \frac{4}{3} t_0^{1/3} s \frac{\partial \rho}{\partial s} \\ \frac{\partial}{\partial s} (\rho \mu^2 + \rho \phi) &= \frac{4}{3} t_0^{1/3} s \frac{\partial(\rho \mu)}{\partial s} \\ \frac{\partial}{\partial s} \left(\frac{5}{2} \rho \phi u + \frac{1}{2} \rho \mu^3 - \left(\frac{\kappa_0}{t_0^{4/3}} \right) \phi^{5/2} \frac{\partial \phi}{\partial s} \right) &= \frac{4}{3} t_0^{1/3} s \frac{\partial}{\partial s} \left(\frac{3}{2} \rho \phi + \frac{1}{2} \rho \mu^2 \right)\end{aligned}$$

As expected, all quantities are now a function of one variable, s , instead of two, x & t . Further simplification can be achieved by defining a re-scaled spatial co-ordinate $z = 4s t_0^{1/3}$ and defining new quantities, J_1 , J_2 & J_3 :

$$J_1 = \rho(\mu - z)$$

$$J_2 = \rho\mu^2 + \rho\phi - z\rho\mu$$

$$J_3 = \frac{5}{2}\rho\phi\mu + \frac{1}{2}\rho\mu^3 - \frac{3z}{2}\rho\phi - \frac{z}{2}\rho\mu^2 - \left(\frac{4\kappa_0}{3t_0}\right)\phi^{5/2}\frac{\partial\phi}{\partial z}$$

J_1 , J_2 & J_3 are the self-similar equivalents of fluxes in mass, momentum and energy. The self-similar equations simplify to:

$$\frac{\partial J_1}{\partial z} = -\rho \quad ; \quad \frac{\partial J_2}{\partial z} = -\rho\mu \quad ; \quad \frac{\partial J_3}{\partial z} = -\frac{3}{2}\rho\phi - \frac{1}{2}\rho\mu^2$$

$$\left(\frac{4\kappa_0}{3t_0}\right)\phi^{5/2}\frac{\partial\phi}{\partial z} = 2J_1\phi + \frac{1}{2}J_2\mu - J_3 - \frac{1}{2}zJ_1\mu + \frac{1}{2}zJ_2$$

where ρ & μ are calculated from the equations for J_1 & J_2 .

$$\mu = \frac{1}{2}\left(\frac{J_2}{J_1} + z\right) \pm \frac{1}{2}\left[\left(\frac{J_2}{J_1} - z\right)^2 - 4\phi\right]^{1/2} \quad ; \quad \rho = \frac{J_1}{\mu - z}$$

We now see that not only are all quantities functions of z alone, but there is only one numerical constant, κ_0/t_0 . This constant determines the ratio of energy flux by thermal conduction to energy flux by hydrodynamic motion and whether the solution lies in the ablative or heat flow regime.

The difficulty in solving the above equations lies in the transition through a special point, which is the equivalent of the sonic point in steady ablation, where \pm changes sign in the equation for μ . So we find a solution by reverting to the time dependent equations and solving them for a laser intensity which grows linearly in time and deposits all its energy at a particular density ρ_{abs} . It is straightforwardly established that at time $t = 0$, the self-similar solution consists of a discontinuous density jump between two uniformly dense zero-temperature regions in which $\rho > \rho_{abs}$ or $\rho < \rho_{abs}$ in the overdense or underdense plasma respectively. By integrating the equations forward in time we obtain the self-similar solution. By solving the equations in dimensional units the solution is easily related to real laser and target parameters. The numerical constant κ_0/t_0 is determined by the choice of the rate at which the laser intensity increases. The top three panels in figure 1 show how the laser-plasma interaction changes from the ablation regime at an absorbed laser intensity at 10^{15}Wcm^{-2} to a supersonic electron heat front at 10^{17}Wcm^{-2} . The results at 10^{16}Wcm^{-2} lie between the two regimes. At all three intensities the laser wavelength is $1/3\mu\text{m}$ and absorption takes place at the critical density. The dense part of the target, at the right hand boundary, is initialised at 1 gm cm^{-3} . The laser intensity rises linearly in time to reach the specified intensity at the end of a laser pulse of duration τ . The total laser energy is made the same at each laser intensity by choosing a pulse duration inversely proportional to the laser intensity such that in the left hand graph in the figure the intensity reaches

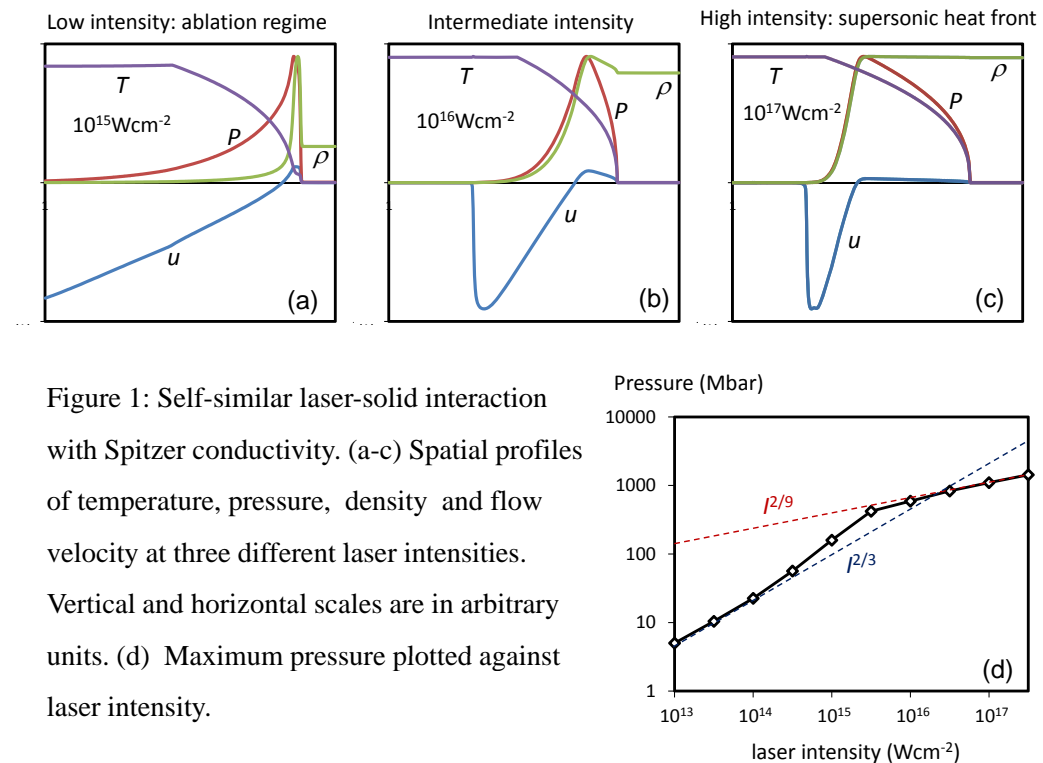


Figure 1: Self-similar laser-solid interaction with Spitzer conductivity. (a-c) Spatial profiles of temperature, pressure, density and flow velocity at three different laser intensities. Vertical and horizontal scales are in arbitrary units. (d) Maximum pressure plotted against laser intensity.

10^{15} Wcm^{-2} after 100 psec, whereas in the right hand graph the intensity reaches 10^{17} Wcm^{-2} after only 1 psec. At 10^{15} Wcm^{-2} , the base of the temperature front coincides with the surface of the high density plasma. The high pressure launches a shock into the dense plasma and causes plasma to ablate from the surface. In contrast at 10^{17} Wcm^{-2} , the temperature front penetrates supersonically into the dense plasma with very little time for the plasma to start expanding from the surface. The lower plot in figure 1 displays the variation of the maximum pressure with laser intensity. At low intensity, the maximum pressure is proportional to laser intensity to the power $2/3$ as expected for the ablation regime. At high intensity, the pressure is proportional to intensity to the power $2/9$ as can easily be derived for a supersonic electron heat front. Figure 1 indicates that shock ignition lies at about the transition point between the two regimes, although the complicated density structures at the end of the compression phase must be taken account of for a realistic calculation, and non-local transport may affect the results.

References

- [1] R. Betti et al. Phys Rev Lett **98**, 155001 (2007); R. Betti et al JPhys conf series **112**, 022024 (2008)
- [2] X. Ribeyre et al. Plasma Phys Cont Fusion **51**, 015013 (2009)